[redacted]

Copy 196
RM L54G28a

RESEARCH MEMORANDUM

FREE-FLIGHT DETERMINATION OF FORCE AND

STABILITY CHARACTERISTICS OF AN INCLINED BODY OF FINENESS

RATIO 16.9 AT A MACH NUMBER OF 1.74

By Warren Gillespie, Jr.

Langley Aeronautical Laboratory
Langley Field, Va.

NATIONAL ADVISORY COMMITTEE FOR AERONAUTICS

WASHINGTON
November 15, 1954

[redacted]

NATIONAL ADVISORY COMMITTEE FOR AERONAUTICS

RESEARCH MEMORANDUM

FREE-FLIGHT DETERMINATION OF FORCE AND STABILITY CHARACTERISTICS OF AN INCLINED BODY OF FINENESS RATIO 16.9 AT A MACH NUMBER OF 1.74

By Warren Gillespie, Jr.

SUMMARY

The force and stability characteristics of a body of fineness ratio 16.9 were determined in free flight at a Mach number of 1.74 and a Reynolds number of 94×10^6. The test results compare favorably with a wind-tunnel test of a similar body and with calculations by the method presented by Allen in NACA RM A9I26 for estimating the effects of viscosity on an inclined body of revolution. When the boundary layer is turbulent and the crossflow drag coefficient corresponding to a yawed circular cylinder is used, the method presented by Kelly in Naval Ordnance Test Station TM-998, which assumes the crossflow to be in a transient state of development along the body, overestimates the viscous body lift.

INTRODUCTION

As part of a general program to determine the aerodynamic characteristics of wing-body-tail combinations at supersonic speeds, a rocket-propelled body-alone configuration was flight-tested at the Langley Pilotless Aircraft Research Station at Wallops Island, Va. A second purpose of the test was to fly an inclined body in the critical Reynolds number range wherein the selection of the correct value of the crossflow drag coefficient required for the estimation of the viscous lift and moment acting on an inclined body is uncertain. Previous estimates by the method of reference 1 using crossflow drag data from tests of cylinders at 90° to the free-stream direction have shown relatively poor agreement with experimental body tests in this range.

The body used for this investigation had a fineness ratio of 16.9 and a straight tapered afterbody with a base diameter to maximum body

diameter ratio of 0.71. Lift, drag, and aerodynamic-center location were determined only at a Mach number of 1.74 since either the normal and transverse accelerometer or the angle-of-attack instrument range was exceeded at other Mach numbers which occurred during coasting flight of the model. The Reynolds number of 94 × 10^6 at Mach number 1.74 placed the test well up into the region of turbulent-boundary layer. The data have been analyzed and compared with two different methods for estimating the lift of an inclined body. In making this comparison, crossflow drag data obtained from tests of inclined cylinders reported in reference 2 were used. Since viscous crossflow data in the critical Reynolds number range is rather meager, the results of this initial test may be of general interest and are reported at this time.

SYMBOLS

a_n normal acceleration, g units

a_t transverse acceleration, g units

a_l longitudinal acceleration, g units

α angle of attack, deg

β angle of sideslip, deg

p_b base pressure, lb/sq in.

a_r resultant of normal and transverse accelerations, $|a_r| = \sqrt{a_n^2 + a_t^2}$, g units

α_r resultant of pitch and sideslip angles, $|\alpha_r| = \sqrt{(\alpha)^2 + (\beta)^2}$, deg

φ angle whose tangent is α/β, deg

$\ddot{\theta}_n$ pitching acceleration, radians/sec^2

$\ddot{\theta}_t$ yawing acceleration, radians/sec^2

$\ddot{\theta}_r$ resultant of pitch and yaw angular accelerations, $|\ddot{\theta}_r| = \sqrt{\ddot{\theta}_n^2 + \ddot{\theta}_t^2}$, radians/sec^2

[redacted]

C_N	normal-force coefficient, $\frac{Wa_{n_{cg}}}{qS}$
C_R	resultant-force coefficient, $\frac{Wa_r}{qS}$
C_C	longitudinal-force coefficient, $\frac{-Wa_l}{qS}$
C_L	lift coefficient, $C_R \cos \alpha_r - C_C \sin \alpha_r$
C_D	drag coefficient, $C_C \cos \alpha_r + C_R \sin \alpha_r$
C_m	moment coefficient, $\frac{I\ddot{\theta}_r}{qSd}$
V	model velocity, ft/sec
M	Mach number
g	acceleration due to gravity, 32.2 feet/sec^2
q	flight dynamic pressure, lb/sq ft
W	weight of model, lb
S	maximum cross-sectional area of the body, 0.267 sq ft
I	model pitching or yawing inertia, slug-ft^2
l	body length, 9.85 ft
d	maximum body diameter, 0.583 ft
x	distance of center-of-pressure location from base, ft

Subscripts:

cg	at the center of gravity
b	base

MODEL

A body similar to the body of reference 3 but with a 2-inch longer cylindrical midsection was flown without stabilizing fins. A drawing of the test configuration is shown in figure 1. The overall fineness ratio of the model was 16.9. Fineness ratios of the nose and boattailed sections were 3.6 and 3.9, respectively. The ratio of the base diameter of the 2° straight-tapered afterbody to the maximum body diameter was 0.71. Ordinates defining the nose contour are listed in table I. Model photographs are presented in figure 2.

The model was of metal construction and carried five pulse rockets of approximately 20 lb-sec impulse in addition to a ten-channel telemeter with angle-of-attack, pressure. and accelerometer instruments. However, one channel did not function.

The model and its booster are pictured in the launching attitude in figure 3. Total impulse was approximately 34,000 lb-sec for the two solid-fuel Deacon rocket motors.

TEST

Description.- Low-speed wind-tunnel tests ($M \leqq 0.1$) of a 1/4-scale model of the flight model were first made to determine the feasibility of testing the body configuration in free flight. The tests were made with one and with two degrees of freedom, the latter case simulating combined pitching and yawing of the flight model. With the body center of gravity at the point of rotation well forward and with two degrees of freedom, the 1/4-scale model experienced sustained oscillations which did not damp. With one degree of freedom, the oscillations damped quickly and the model trimmed to about ±10 or ±15°, depending on the pivot location.

The flight model center of gravity was positioned at 0.72 body length from the base such that at zero and small angles of inclination the aerodynamic center was ahead of the center of gravity. At higher angles due to viscous cross forces, the aerodynamic center moved rearward of the center of gravity and the model became statically stable.

Measurements.- The quantities measured by the telemeter system were three normal accelerations, two transverse accelerations, one longitudinal acceleration, angle-of-attack, free-stream total pressure, and model base pressure. The velocity obtained from Doppler radar was used in conjunction with tracking radar and radiosonde data to calculate the Mach number, Reynolds number, and dynamic pressure of the test. The

telemetered free-stream total pressure was not used since radar data were available for determination of the test conditions.

Aerodynamic coefficients were determined at a Mach number of 1.74 and a corresponding Reynolds number per foot length of 9.6×10^6. Data at Mach numbers above 1.74 were not obtained because the ranges of the normal and transverse accelerometers were underestimated and the acceleration traces recorded on the telemeter record between the stop limits were questionable. Below Mach number 1.74, firing of the pulse rockets and lack of aerodynamic damping appears to have caused the angle of attack to exceed the negative stop limit of the flow indicator. The coefficients are based on the body maximum cross-sectional area of 0.267 square foot. The method of data reduction is explained in the appendix.

ACCURACY

The random error in the data is indicated by the scatter of the experimental points. The maximum absolute accuracy of a quantity obtained from a single instrument is usually better than 2 percent of the total calibrated instrument range. The probable error is approximately 1 percent. Presented below are the ranges of the telemeter instruments used in the test model:

Nose angle-of-attack indicator, deg	−13 to +15
Normal accelerometer at the nose, g units	±8
Normal accelerometer near the center of gravity, g units	±10
Normal accelerometer near the base, g units	±12
Transverse accelerometer near the center of gravity, g units	±9
Transverse accelerometer near the base, g units	±10
Longitudinal accelerometer, g units	+1 to −10
Free-stream total pressure, lb/sq in. (gage)	0 to 115
Base pressure, lb/sq in. (gage)	0 to −12

RESULTS AND DISCUSSION

The model attained a maximum Mach number of 2.5 and oscillated continuously in pitch and yaw during coasting flight to lower Mach numbers. However, data were obtained only at a Mach number of 1.74. At this Mach number, the aerodynamic characteristics of the model are primarily due

to angle-of-attack variation since accelerations measured in the transverse direction were small. At Mach numbers above 1.74, the ranges of the normal and transverse accelerometers were alternately exceeded. At Mach numbers below 1.74, the angle of attack exceeded the negative limit of the flow indicator. In the figures presenting data, the flagged symbols indicate that the model angle of attack is decreasing. An hysteresis effect is apparent between the ascending and descending values.

Drag.- The drag polar obtained at Mach number 1.74 is presented in figure 4. The total and base drag coefficients are plotted. With a change in lift coefficient from 0.18 to 1.19 there was a small increase in base drag from a value of 0.09 to 0.11. The base drag was 31 percent of the total drag at a lift coefficient of 0.20.

Lift.- The nonlinear variation of lift coefficient with resultant angle of inclination at Mach number 1.74 is shown in figure 5. The lift characteristics of the present test model are very similar to those of model number 3 of reference 4, tested at a slightly higher Mach number of 1.79.

Figure 6 presents a comparison of theory and experiment for the variation of normal-force coefficient with angle of attack. In applying the method of reference 1 to the present test model, the nonlinear lift due to viscous cross forces for the case of a turbulent boundary layer was added to the linear lift obtained from the first-order theory of reference 5. In calculating the viscous lift, a crossflow drag coefficient of 0.8 was used. This value was selected after inspection of the data presented in figure 10 of reference 2, which show that the supercritical drag coefficient of a circular cylinder increases as the angle of inclination to the free stream becomes less than 90°. The value of 0.8 used here is approximate, since the data of reference 2 do not cover the low angle-of-attack range of the present test; however, it is believed that use of a value less than 0.8 would be incorrect. The total normal-force coefficient thus obtained agrees very well with the experimental data. The theory of reference 6, although strictly applicable only for cylindrical afterbodies, was also applied to the slightly boattailed test body. This theory assumes the crossflow to be in a transient state of development along the body, whereas the method of reference 1 assumes a steady state. For this body the theory of reference 6 overestimated the lift. However, when used with the crossflow drag coefficient suggested therein (0.35 instead of 0.8) the theory of reference 6 estimates with fairly good agreement the experimental normal-force coefficients obtained from the present test. This agreement may be fortuitous since for the case of a turbulent boundary layer the value of 0.35 applies only for a cylinder at 90° to the free stream. Reference 2 indicates that for inclined cylinders at low angles of attack a value of about 0.8 or greater should be used. The theory developed in reference 6, therefore, overestimates the viscous body lift when the boundary layer is turbulent and a more appropriate value of crossflow drag coefficient is used.

Center of pressure.- The experimental center-of-pressure variation with angle of attack is compared in figure 7 with the experimental results for model 3 of reference 4 and with the theory of reference 1 for the test body. The more rearward location of center of pressure for the model of reference 4 may be due in part to the higher fineness ratio nose on that model. Using the theory of reference 1, the center-of-pressure location was calculated, assuming 100 percent boattail pressure lift effectiveness at low angles of attack and 50 percent at higher angles of attack. Since the flow at higher angles should be separated over the top side of the afterbody, the assumption of 50 percent pressure lift effectiveness for the boattail seemed reasonable, and gave good agreement with the experimental points. With the center of gravity at a location of 0.72 body length from the base, figure 7 indicates that the test model had a trim point at an angle of 11.7°.

CONCLUDING REMARKS

Data obtained for a body of fineness ratio 16.9 in free flight at a Mach number of 1.74 lead to the following observations:

1. The test results compare favorably with a wind-tunnel test of a similar body and with calculations by the method of Allen presented in NACA RM A9I26 for estimating the effects of viscosity on an inclined body of revolution.

2. When the boundary layer is turbulent and the crossflow drag coefficient corresponding to a yawed circular cylinder is used, the method presented by Kelly in Naval Ordnance Test Station TM-998, which assumes the crossflow to be in a transient state of development along the body, overestimates the viscous body lift.

Langley Aeronautical Laboratory,
National Advisory Committee for Aeronautics,
Langley Field, Va., July 16, 1954.

APPENDIX

DATA REDUCTION

The resultant angle of inclination, lift, drag, pitching moment, and aerodynamic center of an inclined body in free flight can be obtained if the model is instrumented to measure the following quantities with respect to a set of normal, transverse, and longitudinal body axes passing through the center of gravity of the model: $a_{n_{cg}}$, $a_{n_{nose\ or\ tail}}$ (or $\ddot{\theta}_n$), $a_{t_{cg}}$, $a_{t_{nose\ or\ tail}}$ (or $\ddot{\theta}_t$), $a_{l_{cg}}$, α, and β. It is then possible to calculate the resultant values a_r, $\ddot{\theta}_r$, φ, and α_r. The corresponding aerodynamic coefficients C_R, C_C, C_L, C_D, and C_m are lastly calculated along with the aerodynamic-center location of the body.

For the present test, the sideslip angle β was not measured. However, at the Mach number of 1.74, the side force measured during the angle-of-attack variation was small. At this Mach number, it was assumed that $\alpha_r = \alpha \frac{C_R}{C_N}$ in order to determine the model drag polar. The variation of normal-force coefficient and aerodynamic center with α were obtained from values of $\ddot{\theta}_n$, $a_{n_{cg}}$, and α.

REFERENCES

1. Allen, H. Julian: Estimation of the Forces and Moments Acting on Inclined Bodies of Revolution of High Fineness Ratio. NACA RM A9I26, 1949.

2. Bursnall, William J., and Loftin, Laurence K., Jr.: Experimental Investigation of the Pressure Distribution About a Yawed Circular Cylinder in the Critical Reynolds Number Range. NACA TN 2463, 1951.

3. Gillespie, Warren, Jr., and Dietz, Albert E.: Rocket-Powered Model Investigation of Lift, Drag, and Stability of a Body-Tail Configuration at Mach Numbers From 0.8 to 2.3 and Angles of Attack Between $\pm 6.5^{\circ}$. NACA RM L54C04, 1954.

4. Cohen, Robert J.: Aerodynamic Characteristics of Four Bodies of Revolution Showing Some Effects of Afterbody Shape and Fineness Ratio at Free-Stream Mach Numbers From 1.50 to 1.99. NACA RM E51C06, 1951.

5. Van Dyke, Milton D.: First- and Second-Order Theory of Supersonic Flow Past Bodies of Revolution. Jour. Aero. Sci., vol. 18, no. 3, Mar. 1951, pp. 161-178.

6. Kelly, Howard R.: The Estimation of Normal Force and Pitching Moment Coefficients for Blunt-Based Bodies of Revolution at Large Angles of Attack. TM-998, U. S. Naval Ord. Test Station (Inyokern, Calif.), May 27, 1953.

TABLE I

CONTOUR ORDINATES OF NOSE

Station, inches from nose	Body radius, inches
0	0.17
.06	.18
.12	.21
.24	.22
.48	.28
.73	.35
1.22	.46
2.00	.64
2.45	.73
4.80	1.24
7.35	1.72
8.00	1.85
9.80	2.15
12.25	2.50
13.12	2.61
14.37	2.75
14.70	2.78
17.15	3.01
19.60	3.22
22.05	3.38
24.50	3.50
25.00	3.50

[redacted]

[redacted]

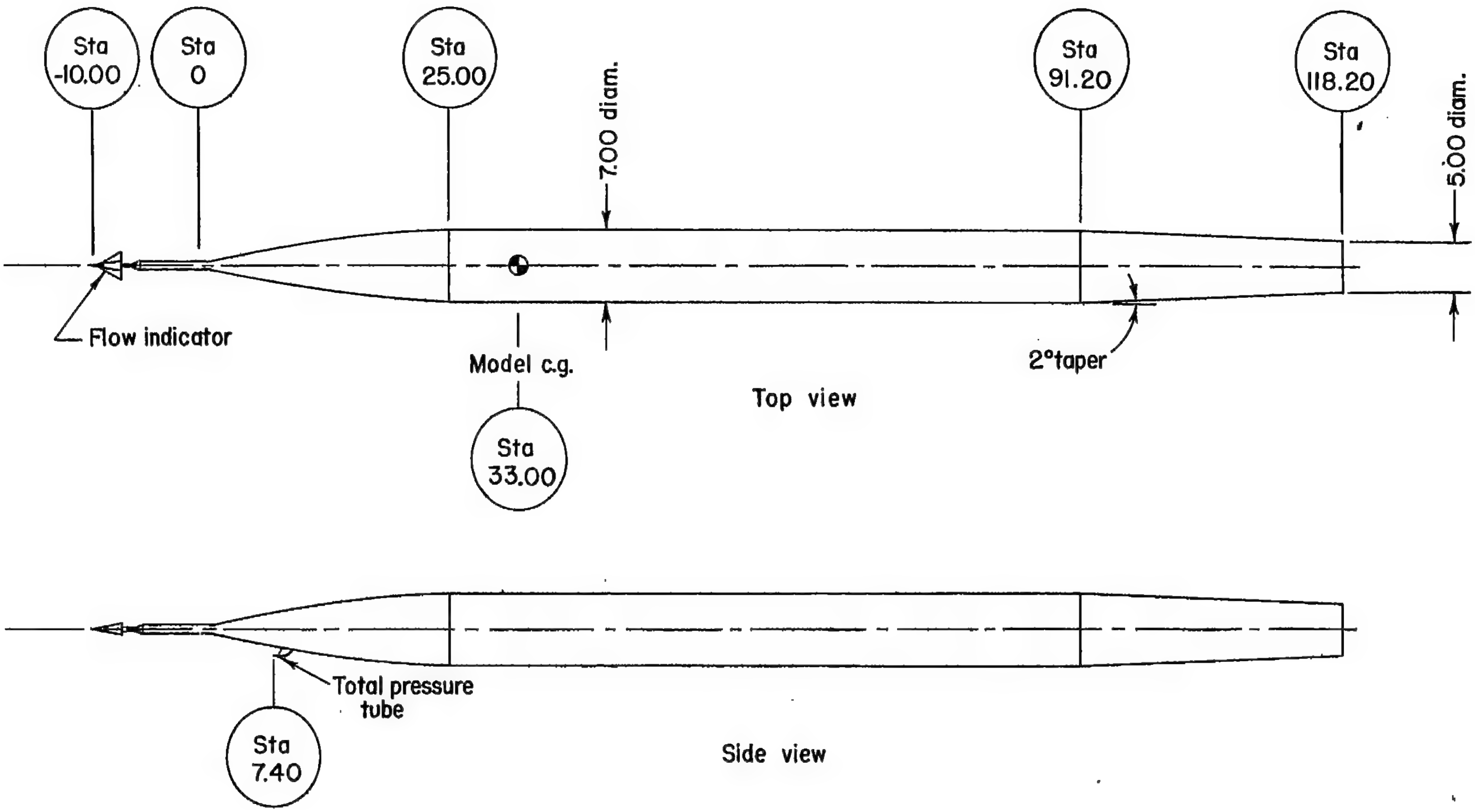

Figure 1.- Two-view drawing of the test configuration. All dimensions are in inches.

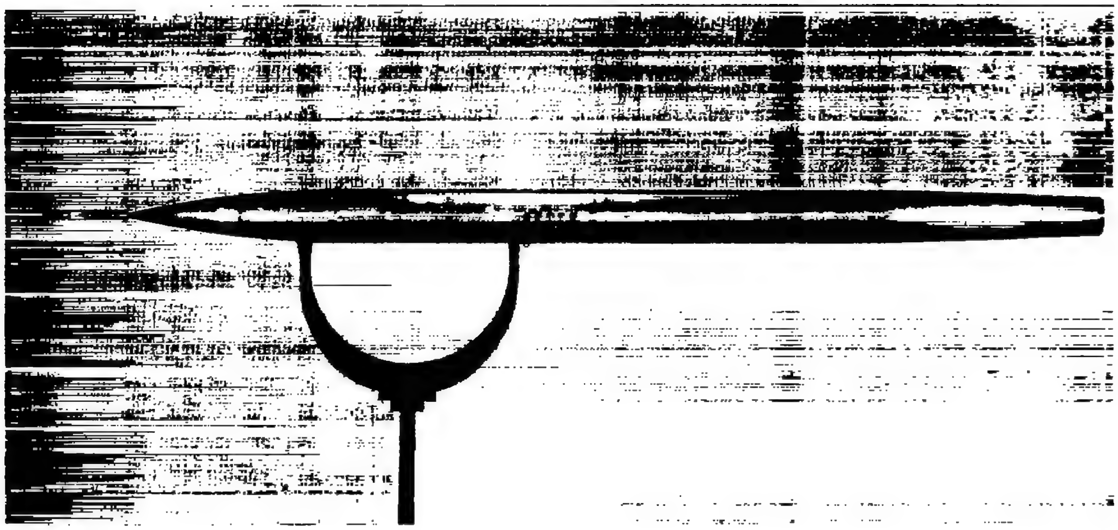

(a) Top view. L-78429.1

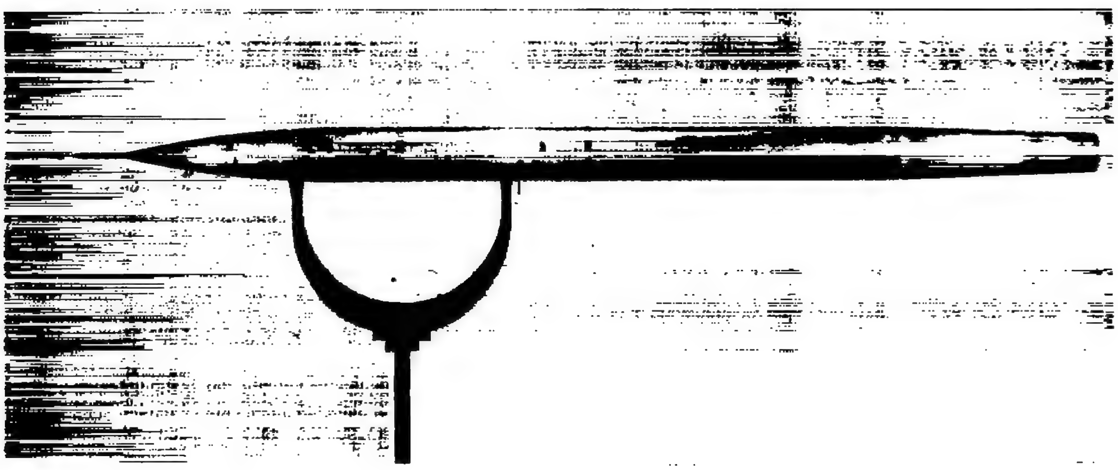

(b) Side view. L-78428.1

Figure 2.- Photographs of the test configuration.

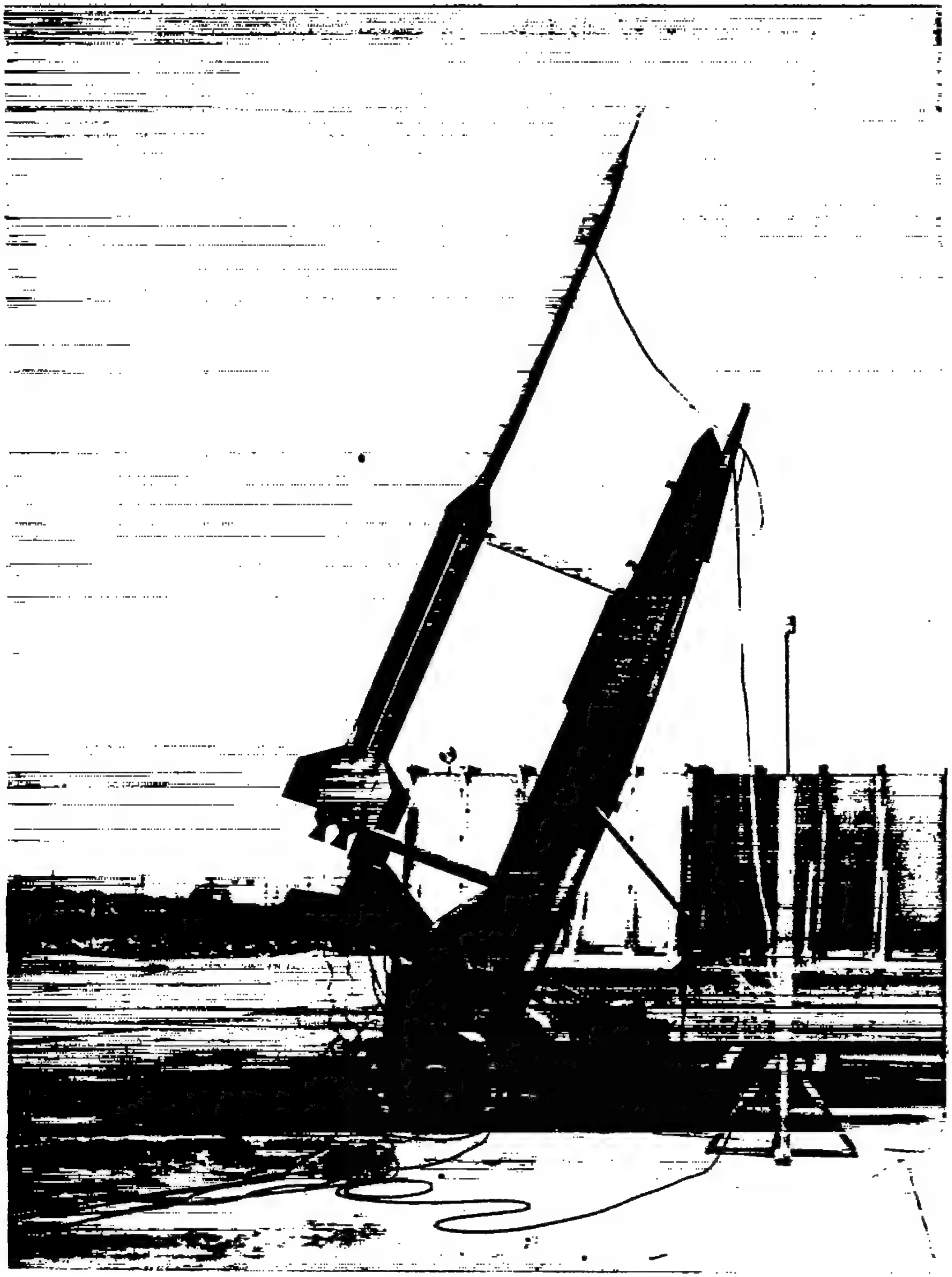

L-78796.1

Figure 3.- Model and booster on launcher.

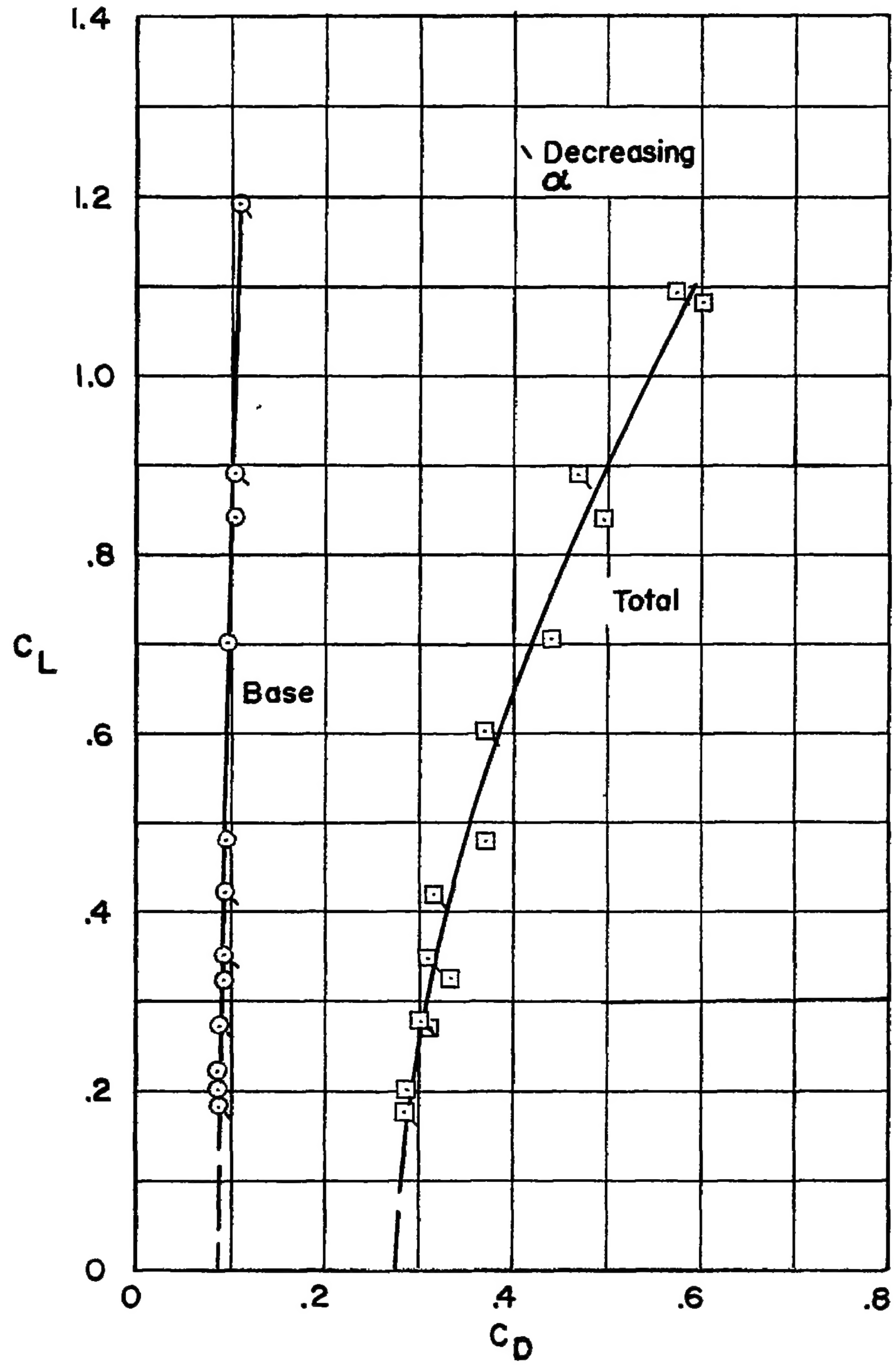

Figure 4.- Drag polar at $M = 1.74$.

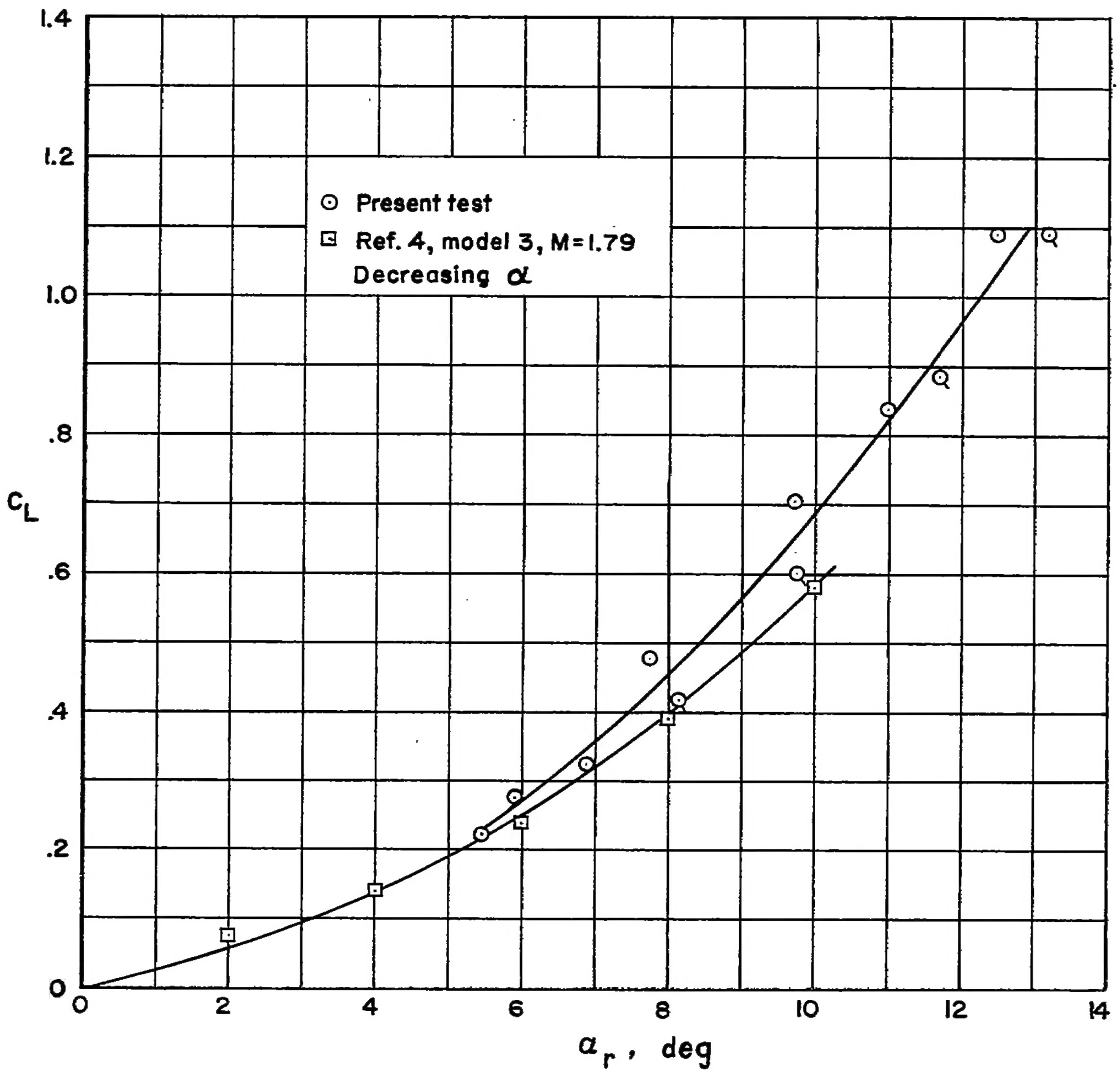

Figure 5.- Variation of lift coefficient with resultant angle of inclination at $M = 1.74$.

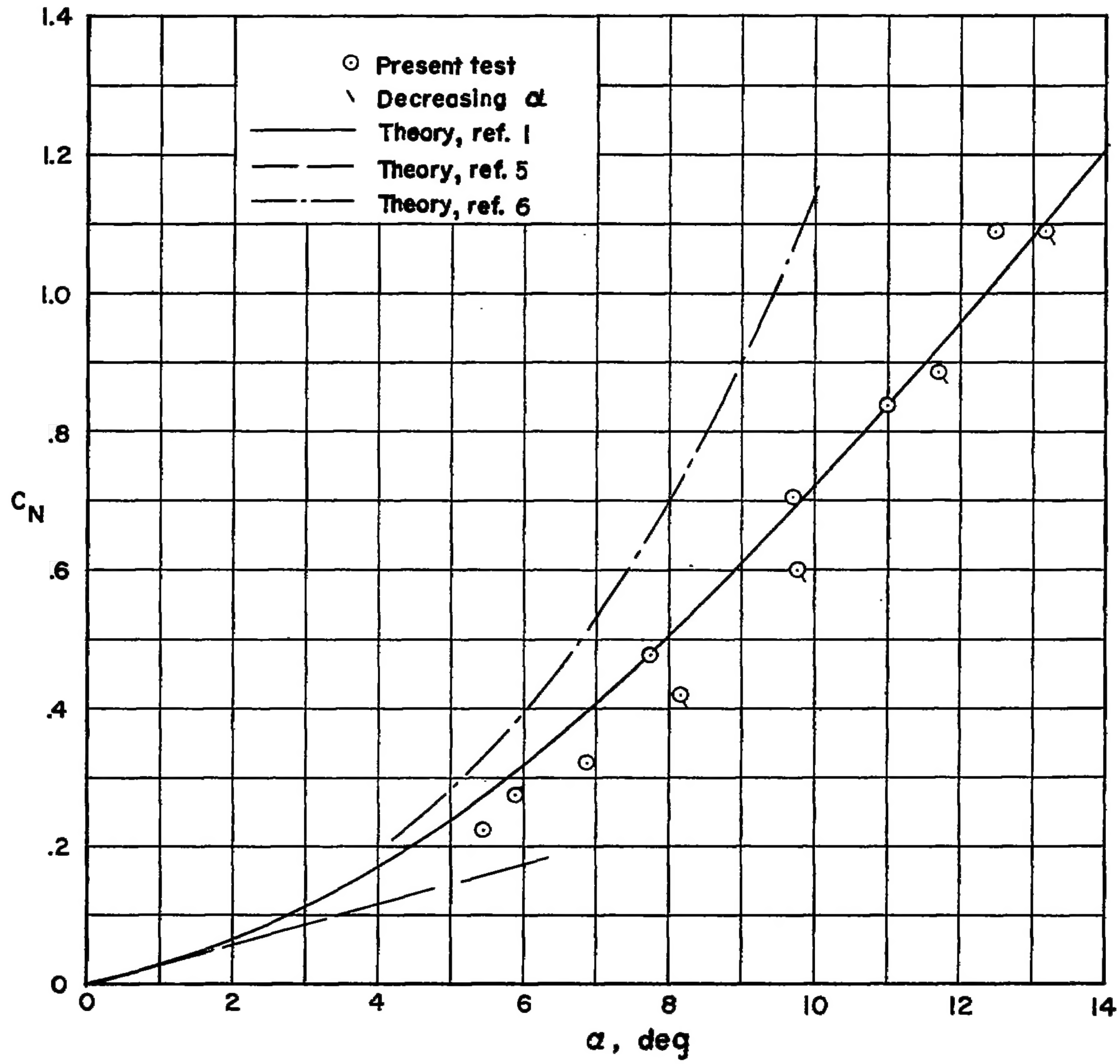

Figure 6.- Comparison of theory and experiment for C_N against α at $M = 1.74$.

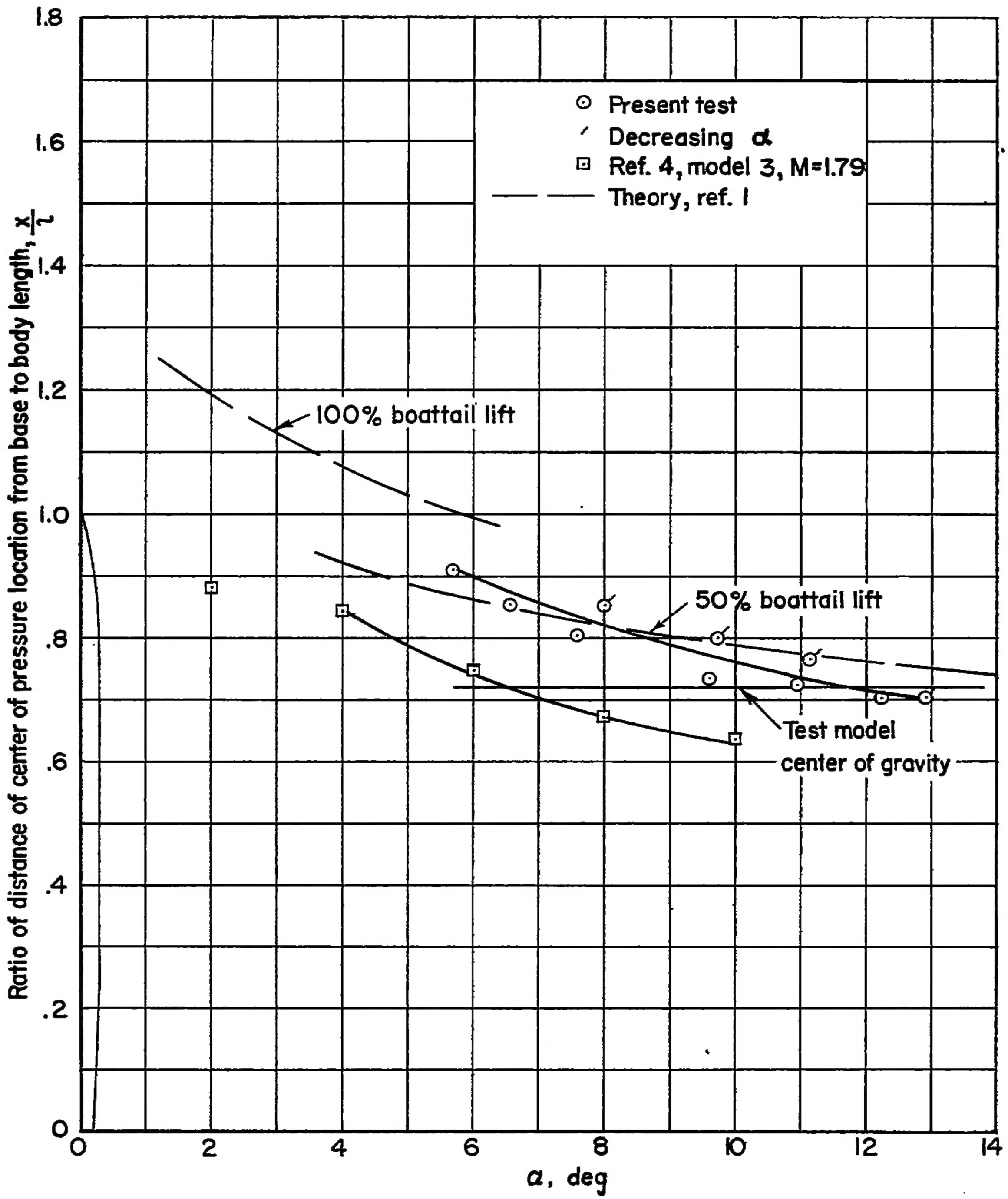

Figure 7.- Center of pressure variation with angle of attack at $M = 1.74$.